THE USE OF A SOLID HYDROCARBON AS A GRAPHITE SUBSTITUTE FOR ASTALOY CrM SINTERED STEEL

T. Pieczonka, J. Georgiev, M. Stoytchev, S.C. Mitchell, D. Teodosiev, S. Gyurov

Dedicated to Dr. Andrej Šalak at the occasion of his 80th birthday.

Abstract

Höganäs Astaloy CrM powder was used to prepare mixtures with 0.3-1.6 % carbon contents, both with and without 1 wt.% manganese additions. The carbon was added in three ways: as a graphite powder, as a solid C_nH_m hydrocarbon powder, and as a mixture of both. Green compacts were pressed at 300 - 800 MPa and sintered isothermally at temperatures in the range 1170 - 1295°C under flowing high purity nitrogen or nitrogen/hydrogen (9:1) atmosphere. Compressibility of the powder mixtures was investigated. Carbon loss occurring during sintering was carefully monitored. Sintering behaviour of numerous combinations of carbon content was investigated by dilatometry. For high carbon contents and high sintering temperatures, densification resulted from controlled generation of a liquid phase. Advantages of using solid hydrocarbon as a carbon donor and of Mn addition in powder metallurgy processing of steels are indicated.

Keywords: sintered structural manganese steel, dilatometry, sintering mechanisms, carbon donor

INTRODUCTION

Carbon plays a fundamental role in iron powder metallurgy [1-7]. As an alloying element carbon strongly determines the principal properties of sintered iron base materials, i.e. their dimensional changes, tensile strength, elongation and hardenability [8-12]. Particularly the latter property is very sensitive to carbon content. For this reason, especially hardenable sintered steels require very careful control of carbon content during the whole production process, i.e. starting from powder mixture (or alloyed powder) till the sintered compact. While the initial carbon content in the green compact can be precisely defined, its final concentration, depending on several materials and processing parameters [13], is not easy to predict. Some help in this matter is given by specially developed diagrams that show the relationships between the equilibrium carbon content in the sintered material at a given temperature, and CO_2 and H_2O contents in the sintering atmosphere. Generally, with regard to carbon control, steels should be sintered in atmospheres with low CO_2 content, a low dew point and with properly chosen carbon potential [14,15]. Obviously, the oxygen concentration in the base powder has a main effect on carbon loss

Tadeusz Pieczonka, University of Science and Technology, Department of Metallurgy and Materials Engineering, Kraków, Poland
Jordan S. Georgiev, Marin Stoytchev, Stojko A. Gyurov, Bulgarian Academy of Sciences, Institute of Metal Science, Sofia, Bulgaria
Stephen C. Mitchell, University of Bradford, Department of Mechanical and Medical Engineering, Engineering Materials Research Unit, West Yorkshire, United Kingdom
Dimitar K. Teodosiev, Bulgarian Academy of Sciences, Institute of Space Research, Sofia, Bulgaria

during sintering when carbon is used for oxide reduction. Therefore, special attention must be paid to the powders used, from the viewpoint of their chemical purity.

Carbon concentration strongly influences the chemical reactions taking place during the sintering cycle, which in turn affect the properties of the sintered material. Thus, to avoid both decarburizing and carburizing and to achieve a proper carbon level in a sintered product, its starting concentration in a green compact must be chosen by taking into account all reactions occurring within a compact, and between it and the sintering atmosphere. Practically, it is best to establish experimentally the relationship of starting vs. final carbon content. In industrial practice the desired concentration of carbon in a green compact may be achieved by using either alloyed or prealloyed powder or a powder mixture containing graphite. The latter option is mostly used because of its versatility in respect to composition and better compactibility. However, there are at least two important disadvantages of graphite containing powder mixtures, i.e. the tendency of segregation during handling and often insufficient homogenization during sintering. To make use of the advantages and to reduce disadvantages of both carbon alloying methods, it can be added partly in the form of fine carbon containing master alloys and partly as graphite. This solution in turn requires a careful control of the master alloy composition, especially when each new batch is made.

To improve dimensional stability by avoiding segregation of graphite in a powder mixture, some organic substances have been introduced recently to iron powder metallurgy [16-21]. Their function is to produce bonded mixtures in which small and light graphite particles are homogenously distributed and do not tend to segregate. There is also the possibility to completely substitute graphite powder with carbon added in a bound form as a hydrocarbon compound [20]. Hydrocarbon compounds have been widely used as hydrogen sources for powering vehicles [22,23]. Particularly, developments of technologies for thermal decomposition of heavy hydrocarbons into high quality fuels are of great interest. Almost in every case, clean carbon is produced as a valuable by-product of the process. The idea in powder metallurgy is to use that carbon to produce sintered steels. Additionally, those organic compounds can also act as lubricants and binders.

Our previous experience of hydrocarbon coating of ceramics and metallic alloys [19,24-27] prompted the use of such techniques for coating ferrous powders. As is well known [28], interactions between metals and hydrocarbons at high temperatures and low pressures cause the hydrocarbon molecules to decompose on the hot metal surfaces. Such a process is accompanied by adsorption of carbon by the metal and the emanation of hydrogen. The purpose of our investigations was to study sintering cycles using dilatometry in order to understand better the reasons for the improvements in sintering and densification of iron-based powders when carbon was added as Carbon-Hydrogen containing Substance (CHS) compared with a graphite addition. While in our previous paper [19] investigating this subject Astaloy 85 Mo Höganäs powder was the base material, for this current paper pre-alloyed Höganäs Astaloy CrM powder was employed. Some microstructures and mechanical properties of similar materials based on Astaloy CrM powder have already been published, as have theoretical phase diagrams [21], now reproduced as Figs. 1 and 2. It should be added, however, that compared with Bain's original work on the effect of chromium on the eutectoid composition, the theoretical diagrams underestimate the carbon content, probably near 0.6 %.

Höganäs Astaloy CrM grade powder seems to be very active, showing significant α-phase sintering during the heating cycle, and this tends to create the problem of oxide vein formation and retention in the sintered microstructure. This is probably due to early pore closure, preventing adequate carbothermic reduction of the chromium oxide. Since graphite diffusion to the metal matrix may not occur fully until the oxides of elements such as chromium have been reduced, significant α-phase sintering can take place before the temperature reaches that of a

α → γ transformation. Thus, the retention of oxide veins is encouraged. Therefore, a modelling study using Thermocalc and MTDATA was performed to investigate ways of reducing this α → γ transformation temperature by other means. Although the addition of 1 % Mn has only a small effect on the solidus temperatures, which is seen in Figs.1 and 2, it does reduce the α → γ transformation temperature by as much as 100°C at lower carbon levels, and thus shows the capability of Mn vapour to reduce the kinetics of CrM [29].

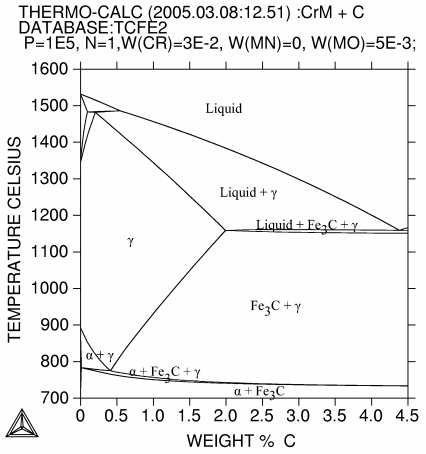

Fig.1. Phase diagram: Astaloy CrM (Fe-3Cr-0.5Mo-C) using TCFE2 database with all carbide phases suspended other than cementite during Thermocalc calculations [21].

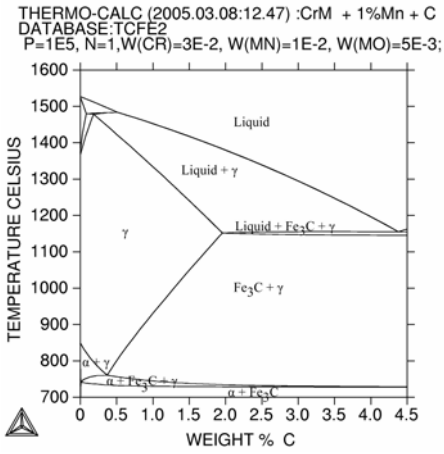

Fig.2. Phase diagram: Astaloy CrM (Fe-3Cr-0.5Mo-1Mn-C) using TCFE2 database with all carbide phases suspended other than cementite during Thermocalc calculations. Note lowered α → γ transformation compared with Fig.1.

Šalak [3] first drew attention to the role of the volatile manganese in the sintering process; the vapour is available from ~650°C. Additionally, it is of course 100 % Mn which means firstly that the concentration of Mn at the sinter neck sites is high, and thus the α → γ transformation temperature near the surface will be reduced very quickly as Mn diffuses. Secondly, Mn vapour is an extremely good getter for oxygen. It reduces oxygen potential at the powder surfaces [3] and has the effect of allowing metal oxides to dissociate. This in turn allows carbon to begin to diffuse a little earlier. This again will ensure the reduction of the α → γ transformation temperature and thus prevent any early pore closure, which means that reducing gases and reaction products can flow in and out of the specimen. This should then improve sintering and densification by a generated liquid phase.

EXPERIMENTAL PROCEDURES

Metal Particles Coating with Carbon-Hydrogen containing Substances (CHS)

Production of carbon-hydrogen substance CHS

Unstabilised polyvinyl chloride (PVC) powder was decomposed in an atmosphere of pure Ar or N_2, by holding for 30 min at temperatures 390-400°C. A black shining substance was obtained; analysis showed only the presence of C and H, which could be represented by the generalised formula C_nH_m.

Coating of metal powders

Three techniques were employed for the coating of Astaloy CrM powder and Astaloy CrM + 1 wt.% Mn (added as an electrolytic powder) powder mixture with CHS (C_nH_m):

Coating from solution - method SE: The C_nH_m powder was milled and then dissolved in toluene (C_7H_8) or benzene (C_6H_6). A subsequent step was the filtration of the solution for the elimination of the insoluble particles. Metallic powder was mixed with some filtrated solution of known concentration of C_nH_m (in our case 44.535 g/l) depending on the required concentration of C in the sintered PM material (Fig.3). The solvent was evaporated under conditions of a continuous stirring of the mixture. This resulted in all the metal particles being coated with a layer of C_nH_m (Fig.4).

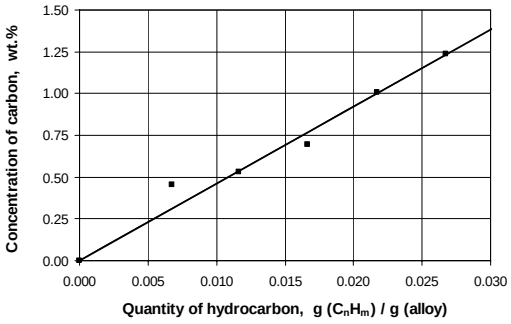

Fig.3. Dependence of carbon content in the sintered compacts as a function of added quantity of CHS.

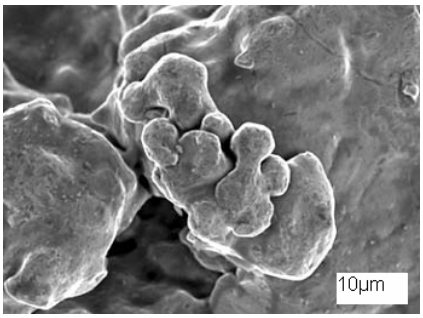

Fig.4. SEM image of Astaloy CrM + 1 % Mn powder mixture coated with CH

S.

Coating from solution and adding graphite - method SE+G: The procedure was the same as SE, but some graphite was added to the metal powder already coated with C_nH_m and the mixture was heated to a temperature of about 100°C in order to ensure the graphite was "glued" to the coating of the metal particles.

Coating without utilizing solvents - method MW: The metal powder was mixed with the powder substance CHS and the mixture was heated to a temperature of <200°C (as the CHS melts in the temperature range of 150-160°C) under conditions of a continuous stirring. Thus the melted substance wetted and coated the metal particles. This method could probably be extended to warm compaction.

Sample preparation

Powder mixtures using Astaloy CrM and pure Mn powder (under 20 µm in size), with different carbon contents, were prepared by three routes. The pressing die was lubricated with liquid paraffin wax. Green density, sintered density and microstuctures were examined on cylindrical (11.3 and 15.0 mm in diameter) samples uniaxially compacted at 300 – 900 MPa. Rectangular (4x4x15 mm^3) samples uniaxially compacted at 600 MPa were also produced for dilatometry investigations. Pressing and sintering parameters for sample preparations and carbon contents in green and sintered compacts are presented in Tab.1.

Tab.1. Compositions and sintering temperatures of Fe-Cr-Mo-[Mn]-C steels based on AstaloyCrM powder, using electrolytic manganese and different carbon donor and amount (using coating methods: SE, SE+G, MW), pressed at 800 MPa.

Coating from solution		
Chemical composition of green compacts	Carbon content [wt.%] after sintering	Isothermal sintering temperature [ºC]
AstCrM- (0.3, 0.5, 0.7, 1.0, 1.24, 1.6) C	0.29-1.58	1170
AstCrM-1Mn-(0.3, 0.5, 0.7, 1.0, 1.24, 1.6)C	0.31-1.58	1170
AstCrM- (0.3, 0.5, 0.7, 1.0, 1.24, 1.6)C	0.31-1,61	1200
AstCrM-1Mn-(0.3, 0.5, 0.7, 1.0, 1.24, 1.6)C	0.28-1.63	1200
AstCrM-(0.3, 0.5, 0.7, 1.0, 1.24)C	0.30-1.24	1240
AstCrM-1Mn-(0.3, 0.5, 0.7, 1.0, 1.24)C	0.30-1.24	1240
AstCrM-1Mn-0.85C	0.875	1280
AstCrM-1Mn-1.00C	0.98	1295

Coating from solution and adding graphite		
Chemical composition of green compacts	Carbon content [wt.%] after sintering	Isothermal sintering temperature [ºC]
AstCrM-1.4C (C_nH_m+0.9%graphite)	1.34	1170
AstCrM-1Mn-1.4C ($C_nH_{m\ 7}$+0.9%graphite)	1.36	1170
AstCrM-1.4C (C_nH_m +0.9%graphite)	1.34	1200
AstCrM-1Mn-1.4C (C_nH_m +0.9%graphite)	1.35	1200
AstCrM-1Mn-1.45C (C_nH_m +0.9%graphite)	1.48	1280

Coating without solvent		
Chemical composition of green compacts	Carbon content [wt.%] after sintering	Isothermal sintering temperature [ºC]
AstCrM-1.6C	1.61	1170
AstCrM-1Mn-1.6C	1.56	1170
AstCrM-1.6C	1.59	1200
AstCrM-1Mn-1.6C	1.57	1200

Sintering

The sintering of the cylindrical compacts was conducted in semi-closed containers in a nitrogen atmosphere having a dew point < -60°C. The sintering cycles were: heat to 400°C at 5°C/min, hold at 400°C for 30 min, heat to 1100°C at 10°C/min, hold at 1100°C for 1 hour, heat to the isothermal sintering temperature (1170-1295°C) at 10°C/min, hold for 1 hour, furnace cool. The rectangular dilatometric samples were sintered in a 9:1 nitrogen/hydrogen atmosphere and cooled at 10°C/min.

EXPERIMENTAL RESULTS AND DISCUSSION

Properties of powders coated with CHS

Some principal technological properties of coated Astaloy CrM powders were assessed. The results of apparent density and flowability are shown in Table 2; for comparison some data for Astaloy CrM powder as delivered are also given. Green density, sintered density and densification of AstCrM + 1 % Mn + 1.45 % C alloy are shown in Table 3. Figure 5 shows the influence of added CHS on green density (GD) of Astaloy CrM and Astaloy CrM + 1 % Mn compacted at 800 MPa. The results are given for powders coated with CHS from solution. Due to the small amount of electrolytic manganese powder added, and its very similar level of density compared with the base powder, its addition did not significantly influence the green density. The green density as a function of compacting pressure for Astaloy CrM + 1 % Mn + 0.88 % C is shown in Fig.6. The powder used for this study was coated with CHS from solution.

Tab.2. Apparent density and flowability of the powder mixtures.

Powder	Apparent density [g.cm^{-3}]	Flow [sec/50g]
Astaloy CrM	2.95	25
Astaloy CrM + 1.45C – method SE	2.69	22
Astaloy CrM + 1.45C (0.95 as C_nH_m and 0.5 as graphite) – method SE+G	2.76	26
Astaloy CrM+ 1.45C – method MW	2.70	33

Tab.3. Green density (GD), sintered density (SD) and densification of AstCrM+1%Mn+ 1.45C alloy sintered at 1280°C.

Compaction Pressure, [Mpa]	GD, [g.cm^{-3}]	SD at 1285°C [g.cm^{-3}]	SD* at 1280°C [g.cm^{-3}]	SD at 1295°C [g.cm^{-3}]	SD* at 1295°C [g.cm^{-3}]	Densifi-cation, % at 1280°C	Densifi-cation,% at 1295°C
300	6.02	7.01		6.96		16.44	15.73
400	6.35	7.23	7.29	7.39		13.86	16.28
600	6.77	7.53	7.7	7.65	7.74	11.23	13.01
800	6.98	7.5	7.57	7.48	7.55	8.45	8.17

SD*- Density measured by hydrostatic method

It is worth noting, that for powders coated with CHS there is nothing to be gained by increasing the compaction pressure from 600 to 800 MPa, because it inhibits densification and thus the sintered density. This is probably because the tighter packing of the powder particles in the latter case prevents the vapour from reaching as many hot metal surfaces, thus limiting production of fine nascent carbon. Furthermore, it will limit powder particle rearrangement during contact with the liquid surface at prior particle boundaries and limit spread of the liquid due to capillary forces, thereby reducing densification. Additionally, the lower porosity is likely to limit manganese vapour transport [3], which in turn reduces the surface activation and alloy evolution. The densification rate may also be lowered due to the increased amount of closed porosity, and a swelling action of gases produced from the hydrocarbon at elevated temperature being unable to flow out the compacts.

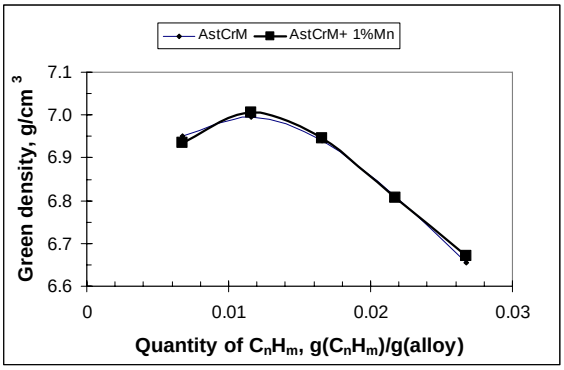

Fig.5. Green densities of Astaloy CrM and Astaloy CrM + 1 % Mn samples as a function of the quantity of C_nH_m addition. Compacting pressure 800 MPa. Powder particles were coated with CHS from solution.

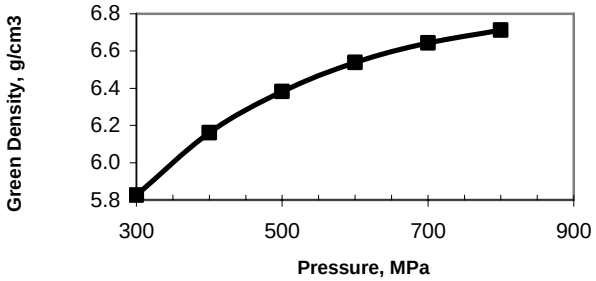

Fig.6. Green density of Astaloy CrM + 1 % Mn + 0.88 % C samples as a function of compacting pressure. Powder particles were coated with CHS from solution.

Sintered compacts produced from powders coated with CHS from solution, ethod SE

All alloys compacted at 800 MPa and sintered at 1170, 1200, and 1240°C exhibit microstructures clearly showing that CHS can be considered as a carbon carrier [21]. Sintering above 1250°C of compositions with high carbon contents involved a liquid phase [21], which promotes densification and homogenisation (Figs.7 and 8). Sintered density vs. compacting pressure, for Astaloy CrM + 1 Mn + 0.88 C specimens compacted at 300 to 800 MPa and sintered at 1280°C, is shown in Fig.9. For this system, the green density increased from 5.80 at 300 MPa to 6.70 g.cm^{-3} at 800 MPa compacting pressure. After sintering the densities ranged from 6.10 to 7.00 g.cm^{-3}, and for pressures above 600 MPa densification was 4 %. There were no significant differences between carbon contents in the green compacts and in the sintered specimens.

The dilatometric traces in Figs.10 and 11 show that the dimensional changes in samples made of powder coated with C_nH_m from solution are greater than those in the samples with only graphite. Furthermore the final dimensional changes, which is shrinkage in each case, in CHS-coated powders are about 3 times larger than that in powders with graphite. Dilatometric curves clearly indicate that the finely-divided nascent carbon coming from the hydrocarbon is more active and covers a larger surface area than graphite, promoting a more uniform diffusion, which moves the $\alpha \rightarrow \gamma$ transformation in iron to lower

temperatures. Additionally, the expansion caused both by temperature increase, but also by carbon diffusion, is lower for CHS-coated powders than that for powder mixtures containing graphite. At the $\alpha \rightarrow \gamma$ transformation points (Fig.11a), it can be seen that the curve for the specimen with graphite addition shows a more diffuse transformation shape, and that the transformation ends at a higher temperature than for the compact containing C_nH_m. Additionally, the traces show that graphite promotes more swelling than C_nH_m (700-1100°C region). This suggests that sufficient carbon is available from the C_nH_m material for alloying the powder particle surfaces, thereby locally lowering the $\alpha \rightarrow \gamma$ transformation temperature. Because of the homogenous distribution of the hydrocarbon substance compared with graphite addition, swelling is minimised.

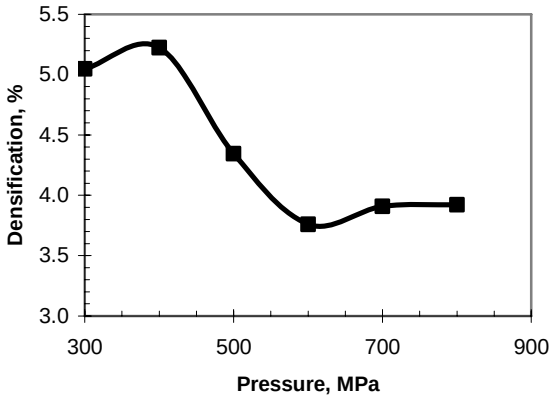

Fig.7. Densification during sintering at 1280°C of Astaloy CrM + 1 % Mn + 0.88 % C samples as a function of compacting pressure. Powder particles were coated with CHS from solution.

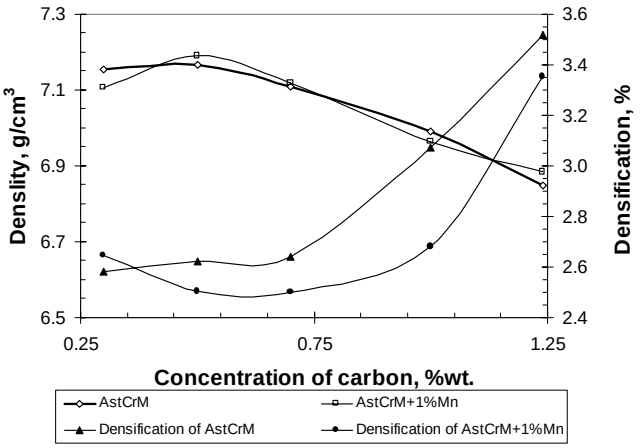

Fig.8. Sintered density (isothermal sintering temperature - 1200°C) and densification of Astaloy CrM and Astaloy CrM + 1 % Mn specimens compacted at 800 MPa as a function of carbon content. Powder particles were coated with CHS from solution.

C_nH_m powder melts, wets of the powder surfaces and will therefore be more homogenous than normal graphite addition. At 1100°C it will have completely dissociated, and its active vapour products are catalysed by the hot metal surfaces to produce the finely divided nascent carbon. This carbon will be well distributed, resulting in higher specific surface due to vapour transport via the porosity. The densification rate during the homogenisation hold for one hour at 1100°C is therefore much greater for C_nH_m than for graphite (Fig.11).

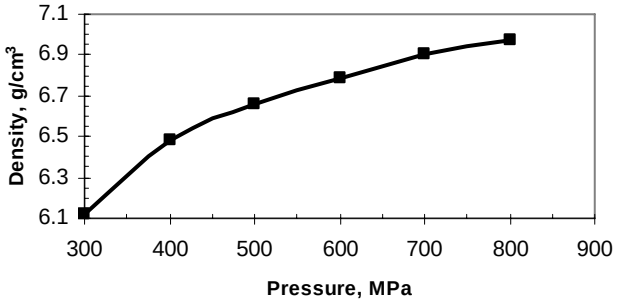

Fig.9. Sintered density (isothermal sintering temperature - 1280°C) of Astaloy CrM + 1 % Mn + 0.88 % C specimens as a function of compacting pressure. Powder particles were coated with CHS from solution.

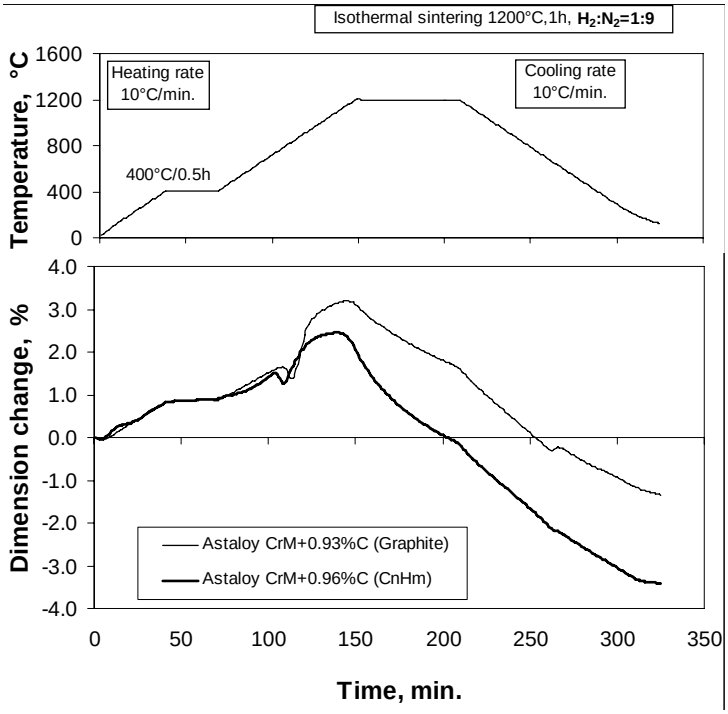

Fig.10. Dilatometric traces for AstCrM + 0.96 % C (coating from solution) and AstCrM + 0.93 % C (graphite) after sintering at 1200°C for 60 min in nitrogen-hydrogen atmosphere 9:1.

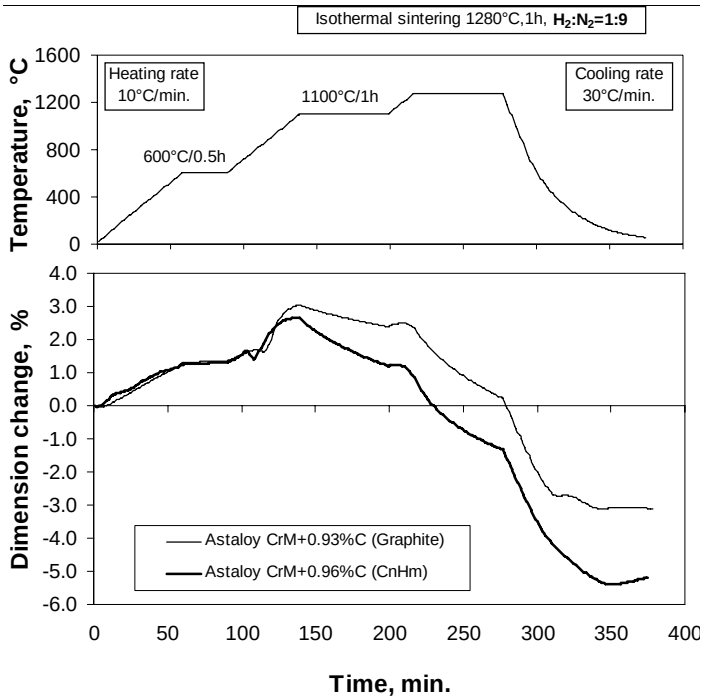

Fig.11. Dilatometric results for AstCrM + 0.96 % C (coating from solution) and AstCrM + 0.93 % C (graphite) after sintering at 1280°C for 60 min in nitrogen-hydrogen atmosphere 9:1.

Furthermore, when analysing the Thermocalc diagrams it may be concluded that the densification that can be seen at 1100°C cannot be attributed to any conventional liquid phase sintering. Therefore, as C_nH_m is not fully dissociated until 1100°C, there will then be a large carbon concentration gradient in this material. This will ensure greater mass transport at 1100°C compared with graphite, which has been free to diffuse over a greater range of temperature and longer time. This greater driving force for mass transport is thus promoting sinter neck growth by volume diffusion, and thereby creating more solid state densification than can possibly occur when using graphite.

During the sintering hold at 1280°C the slopes of the two traces are similar, hence densification rates at this temperature are virtually the same. This is because carbon levels in the two materials will be similar after diffusion during the 1100°C holding period. Since the carbon distribution will be reasonably homogenous at a level of approximately 1 % by weight before the temperature of 1280°C is reached, there is no possibility of forming a liquid phase. This can be seen on Figure 1, where the solidus line for 1 % C is considerably higher than 1280°C, and hence no conventional liquid phase sintering densification mechanism can take place. This emphasises why the slopes of the two traces at 1280°C are virtually identical, regardless of carbon type.

During cooling, the trace (Fig.11) for the specimen with graphite shows a significant bainite transformation, which is not evident for compacts with CnHm. This means that there is a higher positive volume change for the graphite sample compared with CnHm, and hence, lower overall densification. The CnHm graph shows what would appear to be a martensitic transformation around 180°C with a small increase in volume. This martensitic transformation is barely discernible in the graphite sample. Hence we can

deduce that the as sintered carbon level is higher and its distribution probably more homogenous in the CnHm material, which possesses increased hardenability and potential for some sinterhardening.

Sintered compacts produced from powders coated with CHS from solution with adding of graphite, method SE + G

The combined procedure of carbon addition was also used for samples from AstCrM and from AstCrM + 1 % Mn containing 0.5 wt.% C in the form of CHS and 0.9 wt.% C in the form of free graphite. Compacting pressures were 200 - 800 MPa (Table 3) and sintering temperatures 1170, 1200, 1280 and 1295°C. Density after sintering and densification for Astaloy CrM + 1 % Mn + 1.4 % C alloy as functions of green density are shown in Fig.12. The densification of AstCrM + 1 % Mn + 1.4 % C alloy, compacted at 800 MPa, is presented in Fig.13 as a function of the sintering temperature.

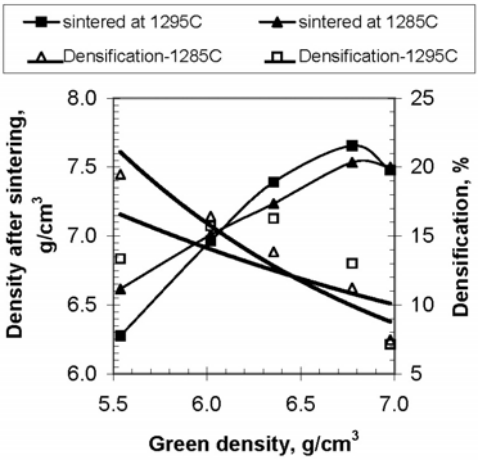

Fig.12. Influence of green density on sintered density and densification for Astaloy CrM + 1 % Mn + 1.45 % C specimens. Coating from solution (0.5 % C) with adding graphite (0.9 % C).

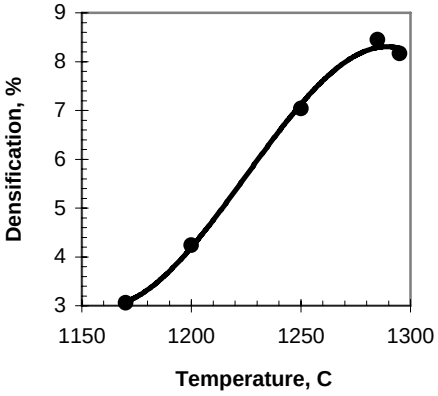

Fig.13. Influence of temperature on densification for Astaloy CrM + 1 % Mn + 1.45 % C specimens compacted at 800 MPa. Coating from solution (0.5 % C) with adding graphite (0.9 % C).

Sintered compacts produced from powders coated with CHS without using solvents method MW

Densification by liquid phase sintering for various high-C alloys is dilatometrically demonstrated in Fig.14. These traces are in accord with the theoretical phase diagrams, indicating that about 1.6 % C is necessary to produce a liquid phase at 1170-1200°C for Astaloy CrM. It should be added that in these as-sintered hypereutectoid alloys, grain boundary carbide networks form [21] at this cooling rate, then a hardening and spheroidisation heat treatment is necessary to obtain the correct combination of strength and toughness.

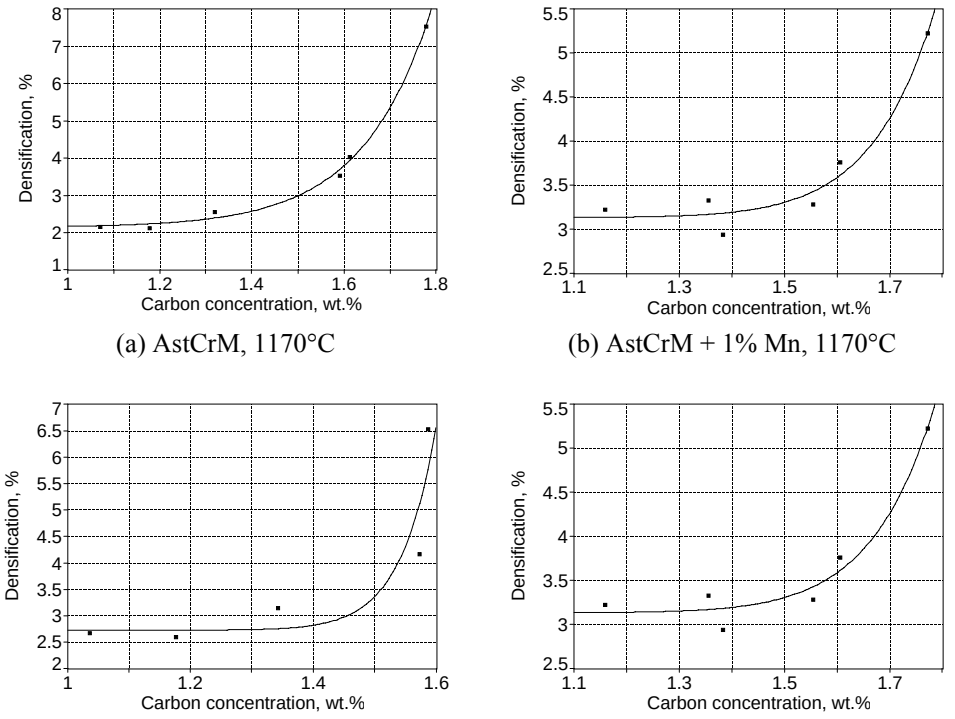

Fig.14. Influence of carbon concentration measured after sintering on densification for Astaloy CrM and Astaloy CrM + 1 % Mn alloys compacted at 800 MPa and sintered at 1280°C.

CONCLUSIONS

Our results show that coating metal powder particles with CHS results in both homogeneous distribution of carbon in the mixture and no segregation between the metal powder and the carbon donor. During the heating period [19] of the sintering cycle CHS fully decomposes up to 1100°C, possibly in a similar way in which CH_4 decomposes [22,23,28] to H, CH-radicals and nascent carbon. Hydrogen and CH-radicals ensure a reducing atmosphere without the use of additional H_2 as a reducing agent. The nascent carbon is adsorbed on the surface of every powder particle, which results in easier diffusion of C into the metal grains, homogeneous distribution of C in the bulk and a homogeneous structure, activating shrinkage more strongly than does graphite. Dilatometry substantiates

that CHS may be considered as a sintering activator. Greater densification of CHS-coated samples is associated with progressive dissociation of the hydrocarbon film and finely, uniformly distributed nascent carbon. Additionally, the use of hydrocarbons as a substitute for the graphite powder in PM iron alloys increases hardenability and potential for sinterhardening. The carburisation process can be advanced if a higher amount of CHS is added. Combination of high carbon content and high sintering temperature results in the formation of a liquid phase, and accordingly, grain boundary carbide networks on cooling.

Presumably the higher C_nH_m content in the coated powder increases the frictional forces during the compaction process, thus decreasing the green density (compared with that of mixes with graphite). In order to remove this disadvantage, the amount of C_nH_m was reduced and some graphite added, for use both as a donor and lubricant. Employing this technique, densities of 7.7 $g.cm^{-3}$ were obtained after sintering at 1285°C for 1.48 % total carbon, i.e. involving liquid phase sintering (see Table 3). The structure of all studied CHS-coated powders after sintering show uniform phase distribution on the cross-sections [21].

Due to carcinogeneity of the solvents benzene and toluene, preference is given to the "dry" technique for coating with CHS without using solvents. Such a "dry" coating process gave promising initial results.

The addition of 1 wt.% manganese improves the sinterability of CrM based materials as it lowers the $\alpha \rightarrow \gamma$ transformation temperature by ~100°C, in accordance with the computer generated phase diagrams (see Figs.1 and 2) [21].

Acknowledgements

The work was partly supported by the Polish Ministry of Science and Informatics at the AGH University of Science and Technology under grant No. 11.11.110.491 and at the University of Bradford and IMS, Sofia by a NATO Science for Peace grant SfP 972395.

REFERENCES

[1] German, RM.: Powder Metallurgy Science. Princeton : MPIF, 1994
[2] German, RM.: Powder Metallurgy of Iron and Steel. New York : J. Wiley & Sons, Inc., 1999
[3] Šalak, A.: Ferrous Powder Metallurgy. Cambridge International Sci. Publ., 1995
[4] Thümmler, F., Oberacker, R.: An Introduction to Powder Metallurgy. London : The Institute of Materials, 1993
[5] Höganäs Handbook for Sintered Components. Vol. 3. Design and Mechanical Properties. Höganäs, 1997
[6] Metals Handbook. Powder Metallurgy. Vol. 7. Metals Park, OH : American Society for Metals, 1993
[7] Schatt, W., Wieters, KP.: Powder Metallurgy. Processing and Materials. EPMA, 1997
[8] Pieczonka, T., Mitchell, SC., Stoytchev, M., Kazior, J. In: PM^2TEC 2001. Advances in Powder Metallurgy & Particulate Materials – MPIF 2001, p. 10-141
[9] Pieczonka, T., Kazior, J., Płoszczak, J. In: Proc. of EURO PM'2001. European Congress and Exhibition on Powder Metallurgy, vol. 1, p. 310
[10] Engström, U. In: Advances in Powder Metallurgy & Particulate Materials, vol. 5, MPIF, 2000, p. 5-147
[11] Berg, S. In: PM^2TEC 2001. Advances in Powder Metallurgy & Particulate Materials – MPIF, 2001, p. 5-18
[12] Mitchell, SC.: The Development of Powder Metallurgy Manganese Containing Low-Alloy Steels. Ph.D. thesis. University of Bradford., 2000
[13] Kremel, S., Raab, C., Danninger, H. In: Proc. of EURO PM'2001. European Congress

and Exhibition on Powder Metallurgy, vol. 1, p. 52
[14] Šalak, A., Selecká, M. In: Proc. Höganäs Chair Workshop Sintering Atmospheres for Ferrous PM Components. Wien : TU, 1999
[15] Danninger, H. In: Proc. Höganäs Chair Workshop Sintering Atmospheres for Ferrous PM Components. Wien : TU, 1999
[16] Larsson, M. In: Advances in Powder Metallurgy & Particulate Materials, vol. 2, MPIF, 2000, p. 2-41
[17] Luk, SH. In: Advances in Powder Metallurgy & Particulate Materials, vol. 3, MPIF, 2000, p. 3-167
[18] Vidarsson, H., Lewenhagen, J., Johansson, B. In: Advances in Powder Metallurgy & Particulate Materials, vol. 3, MPIF, 2002, p. 3-1
[19] Pieczonka, T., Georgiev, J., Stoytchev, M., Mitchell, SC., Teodosiev, D., Gyurov, S. In: Proc. Euro PM2003. Valencia, EPMA, vol. 1, p. 441
[20] Mota, JM., Martin, ME., Gordo, E., Velasco, F., Martinez, MA.: Powder Metallurgy, vol. 47, p. 99
[21] Mitchell, SC., Wronski, AS., Georgiev, J., Stoytchev, M. In: Proc. PM2004, Vienna. World Congress and Exhibition on Powder Metallurgy, vol. 3, p. 313
[22] Muradov, N. In: Proc. 2000 DOE Hydrogen Program Review, NREL/CP-570-28890.
[23] Muradov, N. In: Proc. 2001 DOE Hydrogen Program Review, NREL/CP-570-30535.
[24] Yordanova, M., Teodosiev, D., Georgiev, J.: Acta Morfologica et Antropologica, BAS, vol. 6, 2001, p. 64
[25] Yordanova, M., Teodosiev, D., Georgiev, J.: Acta Morfologica et Antropologica BAS, vol. 6, 2001, p. 71
[26] Georgiev, J., Pieczonka, T., Stoytchev, M.: Surface & Coatings Technology, vol. 145, 2001, p. 101
[27] Teodosiev, DK., Isaev, NV.: Chem. Phys. Reports, vol. 19, 2001, no. 6, p. 1165
[28] From, E., Gebhard, E.: Gase und Kohlenstoff in Metallen. Berlin, Heidelberg, New York : Springer- Verlag, 1976
[29] Mitchell, SC., Wronski, AS., Cias, A., Stoytchev, M.: Advances in Powder Metallurgy and Particulate Materials MPIF, vol. 2, 1999, p. 7-12